ADVANCED MATERIALS INTERFACES
Open Access

Supporting Information

for *Adv. Mater. Interfaces*, DOI 10.1002/admi.202400669

From Microscale to Road Scale: Bridging the Gaps of Predictive Aluminum Corrosion Using SECM

Vikram Singh, Alban Morel, Danick Gallant and Janine Mauzeroll**

From Microscale to Road Scale: Bridging the Gaps of Predictive Aluminum Corrosion using SECM

Vikram Singh[1#], Alban Morel[2*#], Danick Gallant[2], and Janine Mauzeroll[1*]

[1]Department of Chemistry, McGill University, Montreal, Quebec, H3A 0B8, Canada

[2]Automotive and Surface Transportation, National Research Council Canada, Saguenay, Quebec, G7H 8C3, Canada

E-mail: janine.mauzeroll.mcgill.ca; alban.morel@cnrc-nrc.gc.ca

*Corresponding authors

#authors contributed equally

Table of contents:

1. Experimental section

1.1 ***Materials and Chemicals:*** Various chemicals procured included NaCl (⩾ 99.0%, Fisher Scientific, USA), ethylene glycol (EG-OH; 90-100%; ACP Chemical, Canada), and acetic acid (Fisher Chemical; USA). The redox mediators used include Ferrocenemethanol (FcMeOH; 97%; Sigma Aldrich) and Hexaammineruthenium (III) chloride (RuHex; 99%; Sigma Aldrich). To fabricate the carbon fiber microprobe, carbon fiber (CF) was purchased from HEKA, Germany, and the soda lime capillaries (AR8350; L = 70 mm; OD = 1.0 mm; and ID = 0.426 mm) were procured from Hilgenberg, GmbH.

1.2 ***AAxxxx samples:*** AA6061 was purchased from Metaux Profusion (purchased; Quebec, Canada), while AA6111, AA7075, and AA5083 were provided by METALTec members. Prior to the use of any samples, they were degreased and cleaned using acetone followed by further processing in terms of heat treatments, and mechanical surface finish (rolled or grinded). The rolled samples have no mechanical treatment whereas, the grinded samples were sanded using 150-grit paper with an orbital sander.

No surface pre-treatment was employed before any electrochemical measurement.

1.3 ***Applicability of these AAxxxx surfaces used in present study:*** In terms of the larger picture, aluminium alloys are attractive for the original equipment manufacturers (OEMs) given their strength, light weight, formability, and durability for automobile and aerospace applications. Considering these applications, we choose four different Al alloys (AAxxxx) namely AA5083, AA6061, AA6111, and AA7075 with different surface finishes like rolled, grinded, Zr-coated, and ZnPh-coated after a sealer layer to yield the nine differently finished surfaces investigated. All these investigated alloys possess a zirconium or ZnPh coating as it is the current best alternative versus the toxic chromium chemistries. Their alloy-specific applicability is briefly discussed below, however for an elaborate discussion the readers are referred to the reviews by Zheng et al [1] and You et al [2].

- **AA5083:** It is recognized for its performance under harsh environments. Therefore, it is highly suited for marine (like ship building) and chemical industry applications (like pressure vessels).
- **AA6061:** It is a versatile variant known for its heat-treatability making it suitable for heavy-duty structural applications like truck frames, rail coaches, aircraft structure etc.
- **AA6111:** It is typically used as a body-sheet alloy in the automotive sector and incorporates copper (0.5 to 0.9 wt%) in the alloy making it prone to filiform corrosion and hence requires corrosion studies to advance coating strategies.
- **AA7075:** It possesses high strength and hence suitable for stressed structural parts like in aircrafts towards gears, shafts etc.

1.4 ***Coating procedure:*** Zr- and ZnPh-based conversion coatings: Post mechanical and heat treatment, AAxxxx surfaces were coated with Zr or ZnPh at ACT Test Panels following their standard procedure for the automotive industries. Samples having zirconium conversion coating (AA5083, AA6061, AA6111, and AA7075) are represented as AA5083-rolled-Zr, AA6061-rolled-Zr, AA6061-grinded-Zr, AA6111-rolled-Zr, AA6111-grinded-Zr, AA7075-rolled-Zr, and AA7075-grinded-Zr. Likewise, samples with ZnPh conversion coating either with or without sealer are represented as AA7075-rolled-ZnPh-no sealer and AA7075-rolled-ZnPh-sealer.

All the electrochemical measurements were performed on samples without any automotive paint (only conversion coatings) whereas, the road test was performed after automotive paint coating (details are provided below).

For the road test measurements, all the samples were additionally coated with an automotive paint system applied by the ACT Test Panels to ensure the real applicability of these samples in the vehicles/transportation sector. The following combinations were prepared for all the samples along with the automotive paint system where the description of each step is provided further below:

- Bare surface: no conversion coating; only acetone decreased, E-coat, Primer, base, clear
- Zr-based: Zr-conversion coating, E-coat, Primer, base, clear

- ZnPh-sealer: ZnPh, sealer, E-coat, Primer, base, clear
- ZnPh-no-sealer: ZnPh, E-coat, Primer, base, clear

E-coat: ED6060C; Primer: 765224EH-Item 47385; Base: 1370AC301-straight shade white-item 55912; Clear: RK8211-Item 59380.

2. Road test measurements

Road test measurements were conducted on the nine selected aluminum alloy surface finish/conversion coating combination namely, AA5083-rolled-Zr, AA6061-rolled-Zr, AA6061-grinded-Zr, AA6111-rolled-Zr, AA6111-grinded-Zr, AA7075-rolled-Zr, AA7075-grinded-Zr, AA7075-rolled-ZnPh-no sealer, and AA7075-rolled-ZnPh-sealer. The road test measurements meant that the truck carrying the test samples was exposed to outdoor weather conditions even while parked due to outdoor parking. The road test was conducted on Quebec (Canada) roads, with the samples being exposed to in-service conditions from June 2019 to October 2021. While traveling, the truck and hence the samples encountered various weather conditions like rain, snow, and heat depending on the seasons. More detailed weather information during this period (June 2019 to October 2021) can be found on Environmental Canada[3]. All the samples were retrieved only after two years of continuous environmental exposure for further testing in the laboratory.

Testing of these samples post road test were performed by analysing the previously marked scribes (2 per sample), which were 2 inches long each. These scribes were marked in such way that they run through the automotive coating to expose the bare metal underneath. These scribes were made diagonally to the rolling direction of the sample by using a tungsten tip.

3. Electrochemical measurements

3.1 ***<u>Preparation of electrolyte solution</u>:*** The supporting electrolyte solution for all the SECM measurements was 35g NaCl /L of ethylene glycol (EG-OH). The three different SECM maps were obtained in different redox mediators namely, (a) 1 mM FcMeOH solution giving Map 1, and (b) an equimolar (1 mM) solution of RuHex and FcMeOH giving Map 2 & 3 in EG-OH electrolyte with 35g NaCl / L in ethylene glycol (EG-OH). An equimolar mixture of the redox mediator was prepared by adding a known weight of RuHex (2 mM) to a known volume of 1 mM FcMeOH solution in 35g NaCl /L of EG-OH.

Given the high viscosity of EG-OH, these electrolyte solutions were sonicated for 30 minutes to ensure complete solubility.

3.2 ***<u>Microelectrode fabrication</u>:*** Before using the CF to make microprobes, CFs were thoroughly washed with Acetone, followed by a 2% nitric acid solution. Afterward, the fibers were washed with ethanol-water solution until the pH turned neutral, followed by drying them in an oven at 120 °C for 2 h. The carbon fiber (CF; 4.7 um) probe was fabricated as per the previously reported protocol.[4] Typically, a 7-8 cm single CF (purchased from HEKA, Germany) was inserted into a soda lime glass capillary (AR8350; L = 70 mm; OD = 1.0 mm; and ID = 0.426 mm) by attaching one end of the fiber with copper wire using commercially available fast curing glue and inserting it into the capillary. Afterward, a capillary containing CF was placed inside the laser-puller (P-2000; Sutter Instrument Company, USA) followed by connecting both ends of the capillary with an RV8 vacuum pump (Edwards, Canada) and evacuating for 10 minutes. Thereafter, a heating and pulling program (Heat: 240; Fil: 5; Vel: 60; Del: 140; Pul: 70) was applied under a vacuum. This protocol resulted in a single glass seal tip composed of CF. The protruded CF was cut about 2 mm from the tip of the glass micropipette with a fine blade. The electrical connection was established using a Cu-wire with silver epoxy (EPO-TEK H20E, Epoxy Technology, USA) followed by curing it at 120 °C in the oven for 30 minutes. Then the assembly was extended and protected using a larger borosilicate capillary (L= 75 mm; OD= 2.0 mm; ID=1.16 mm) and filled with epoxy. The protruded part of the Cu-wire was cut using a scissor and soldered to a gold

pin at the end for the final connection. After the fabrication, the probes were cleaned using a lapping film, (3M, aluminum oxide, 0.05 µm) to remove the remaining CF and any impurities from the surface. After the polishing step, electrochemical characterization of the fabricated probe was done to see if the electrical connection was established and whether the probe contained any impurities on its surface.

3.3 ***Scanning electrochemical microscopy (SECM) measurements*****:** Once the probe was characterized, SECM measurements were performed using it on all nine Al samples. The details of all the surfaces used in the current study are given in the table 1. The SECM measurements were carried out using an IProScan 3 system (bi-potentiostat model PG680, HEKA, Germany) in a Faraday cage (Acoustic Isolation Novascan Ultracube, Ames, IA, USA) on a vibration-free table (Micro 60 Halcyonics Active Vibration Isolation Platform, Novascan, Ames IA, USA). A three-electrode assembly was employed where CF microelectrode was acting as a working electrode, Ag/AgCl leak-free electrode as a reference electrode, and Pt wire as a counter electrode. The Al sample area of 1 cm^2 was exposed to the electrolyte and kept unbiased (at its OCP). Once the setup was ready, the approach curves were collected to land on the surface in 1 mM FcMeOH redox mediator composed of 35g NaCl /L in EG-OH electrolyte while continuously polarising the tip at 600 mV (FcMeOH→ $[FcMeOH]^+$). A larger area of 1 mm x 1 mm was targeted for mapping in SECM for all nine surfaces at a scan speed of 5 um s^{-1} and at a step size of 5um. A three-map SECM configuration for all nine samples was designed wherein these three maps were collected sequentially one after the other. Map 1 was collected only in 1 mM FcMeOH electrolyte solution while continuously polarising the tip at 600 mV. Once map 1 was finished, RuHex was added to the electrolyte so that an equimolar redox-mediator solution of FcMeOH : RuHex results without disturbing the setup. Thereafter, map 2 was collected while polarizing the tip at 0 mV, which is positive enough to detect any Ru^{2+} species produced in close proximity to the surface. After map 2, map 3 was collected without any change in electrolyte but polarizing the tip at 600 mV instead.

A three-map SECM configuration for all nine samples was designed wherein three maps were collected sequentially one after the other as described below:

- **Map 1:** Surface mapping while polarizing the tip at 600 mV in an electrolyte containing 1 mM FcMeOH redox mediator dissolved in 35g NaCl/L of EG-OH. This imaging potential allows the detection of only surface features without activating corrosion sites.
- **Map 2:** After finishing Map 1, RuHex was added to the electrolyte so that an equimolar redox-mediator solution of FcMeOH : RuHex in 35g NaCl/L of EG-OH results without disturbing the setup. The sequential imagining was performed by polarizing the tip at 0 mV to yield Map 2. This imaging potential is positive enough to detect any Ru^{2+} species generated from corrosion sites produced near the surface thereby imaging corrosion hotspots.
- **Map 3:** After finishing Map 2, sequential imaging was performed by polarizing the tip at 600 mV to yield Map 3 without any change in the electrolyte i.e., in an equimolar FcMeOH : RuHex redox mediator dissolved in 35g NaCl/L of EG-OH. This Map 3 therefore, resulted in a superposition of topographical features (as seen in Map 1) and corrosion hotspots (as seen in Map 2).

To ensure reliability, accuracy and consistency of the SECM results the below mentioned steps were taken:

- To eliminate probe-related disparity (if any), a single probe was used for all the nine samples investigated in this study.
- Collecting cyclic voltammetric response at plastic Petridis
- Typical CV measurements for ensuring the sigmoidal behavior behaviour of the SECM tip was performed before each measurement to ensure the reproducibility of the probe surface and the electrolyte composition. All the CV responses exhibited a stable current in the range of 35- 38 pA in 1 mM FcMeOH redox mediator solution.

All SECM measurements were performed at room temperature (22.5 ± 1°C) under ambient relative humidity. No specific actions were taken to control these parameters during the SECM measurements.

3.4 ***<u>Bulk corrosion measurements</u>:*** The bulk corrosion measurements were performed on each sample using the conventional cell (K0235 Flat Cell, Princeton Applied Research, AMETEK Scientific Instruments, Berwyn, PA, USA) in 5% NaCl aqueous solution of pH 2.8 adjusted with acetic acid. This setup was composed of Al sample substrate as a working electrode (WE; 1 cm^2 exposed area), a saturated calomel electrode (SCE) as the reference, and platinum mesh as the counter electrode. Gamry Ref 600 potentiostat was used to measure the electrochemical response mainly collecting the open circuit potential (OCP), and linear polarization (LP) curves. The LP curves were obtained at a fixed scan rate of 1 mV s^{-1} in the potential range of -0.3 V to +0.3 V vs. OCP. Resistance to polarization was determined as the coefficient of the term of degree 1 in a 6^{th}-order polynomial fitted to the E *vs.* I LP data.

4. Data Processing

4.1 ***<u>Hotspot maxima detection from SECM maps:</u>*** [6-8] SECM maps contain significant information, which requires appropriate processing for obtaining process related insight. The SECM data processing procedure employed in this study utilized Python codes, and the sequential steps taken for this implementation are detailed below:

- The as-measured SECM map was smoothed by applying a moving-average function (window width of 50 points) in the x-direction (which is 5 um).
- The local maxima, which is referred to as 'hotspots' were identified from the smoothed SECM map. This gives information about the number of cathodic corrosion sites on the sample using the 'findmaxima2d' package. The 'noise tolerance' parameter is the only required input parameter in this 'findmaxima2d' package to help find the hotspots from the benign background surface.
- The typical scenario of applying a unique noise tolerance value in the 'findmaxima2d' package would not accurately capture the number of hotspots for each sample. Rather, a noise tolerance value had to be chosen on a sample-by-sample basis. To aid in the choice of this value, the maxima identified for a given noise tolerance value were superimposed on a locally normalized map allowing to visually identify as well as differentiate the local maxima on the SECM map. The role of local normalization is to improve the contrast of local maxima thereby clearly differentiating them from the background. The noise tolerance parameter was iteratively changed until it visually captured the local maxima observed on the locally normalized map in a satisfactory manner.

Applying the 'findmaxima2d' function on the smoothed map rather than on the smoothed and locally normalized map allows for the noise tolerance parameter to conserve a physical meaning, which is a current threshold separating hotspot maxima.

5. Potential sources of errors

<u>During SECM</u>: The plausible sources of error & their mitigation measures are:

1. SECM probe variability
    - A single SECM probe (carbon fibre microelectrode, 4.7 µm) was used to investigate all the nine samples while ensuring appropriate functioning using both the optical microscope and electrochemical testing before each measurement.
2. Electrolyte induced variability over time due to evaporation related concentration changes

- A stable EG-OH electrolyte solution was used to allow for flexibility of corrosion imaging over a larger area without undergoing any concentration changes due to their low vapor pressure.

During Road Test: The plausible sources of error & their mitigation measures are:

1. Road condition variability for different samples
   - All the samples were mounted on the same truck for consistency in environmental exposure conditions.
2. Variation in corrosion arising from sample placement on the truck
   - An overall corrosion influence was tested by placing three different representatives of each sample on the driver side and passenger side, which were evaluated for corrosion characteristics.
3. Variation in corrosion characteristics due to industrial coating disparity
   - All the AAxxxx samples were coated in the same bath at the ACT Test Panels LLC facility.

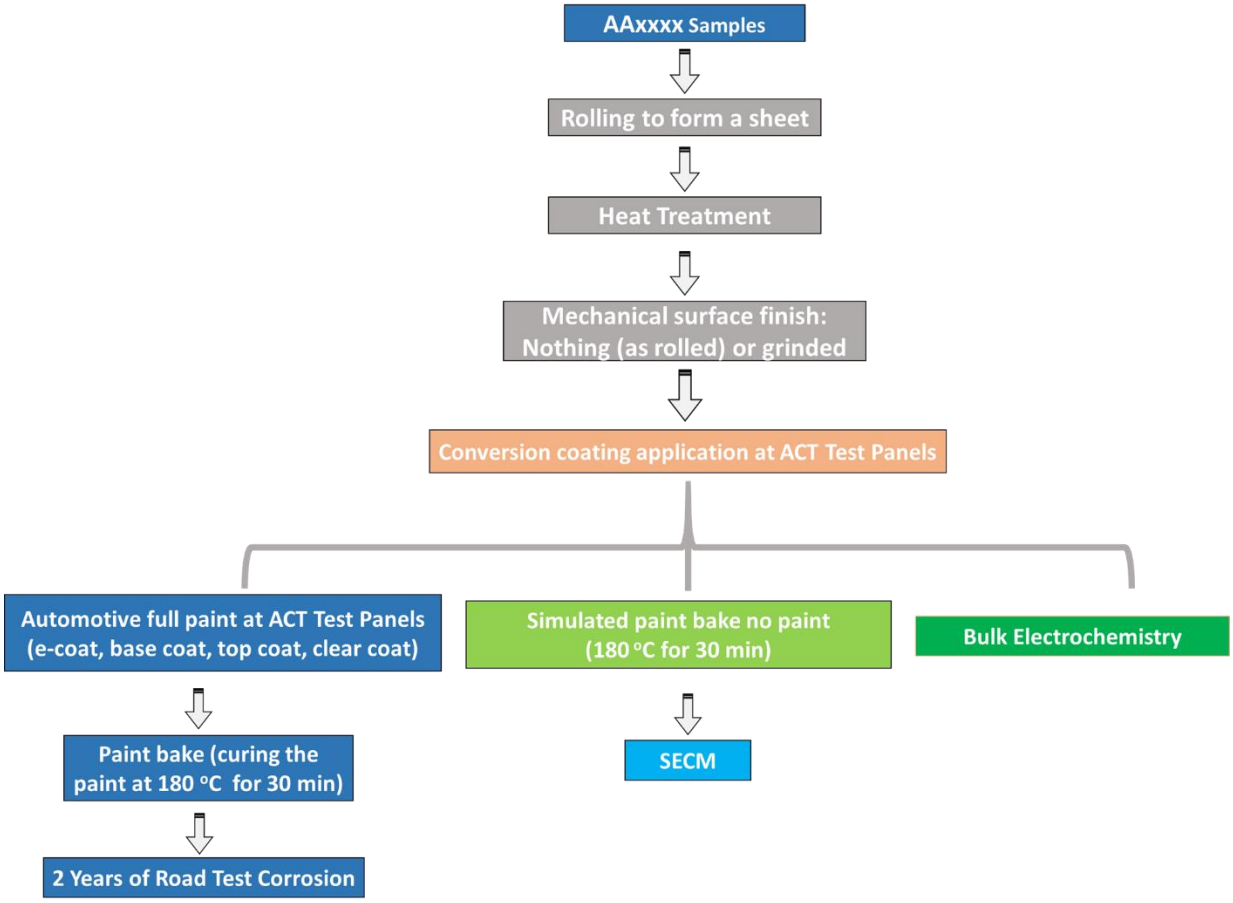

Figure S1. Process flow map for sample preparation and testing of nine differently finished AAxxxx surface.

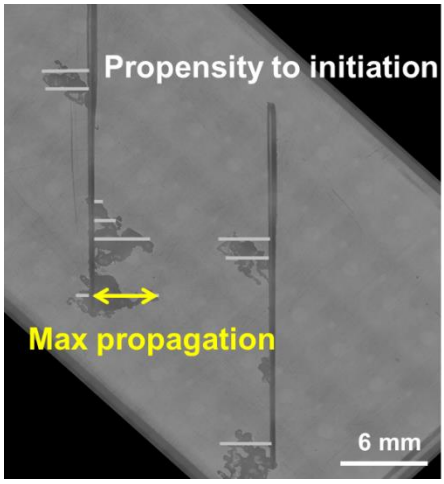

Figure S2. Optical image of a representative sample AA7075-rolled-Zr, showing corrosion islands on the surface. Two scribes marked on the surface is depicted perpendicular to which 20 equidistance lines are typically marked. Propensity to initiation (%) was determined from the number of these lines across the scribe showing corrosion (white lines), whereas the mean length of those lines gives propensity in propagation (mm), and finally, the maximum length of the line (mm) gives corrosion propagation (yellow line).

Table S1. Elemental Compositional (wt %) details of each Al samples used in this study[5]

Sample	Mg	Mn	Si	Ti	Zn	Fe	Cu	Al
AA5083-rolled-Zr	4 - 4.9	0.4 - 1.0	Max 0.4	Max 0.15	Max 0.25	Max 0.4	Max 0.1	Balance
AA6061-rolled-Zr	0.8 - 1.2	Max 0.15	0.4 - 0.8	Max 0.15	Max 0.25	Max 0.7	0.15 - 0.40	Balance
AA6061-grinded-Zr	0.8 - 1.2	Max 0.15	0.4 - 0.8	Max 0.15	Max 0.25	Max 0.7	0.15 - 0.40	Balance
AA6111-rolled-Zr	0.5 - 1	0.15 - 0.45	0.7 - 1.1	Max 0.1	Max 0.15	Max 0.4	0.5–0.9	Balance
AA6111-grinded-Zr	0.5 - 1	0.15 - 0.45	0.7 - 1.1	Max 0.1	Max 0.15	Max 0.4	0.5–0.9	Balance
AA7075-grinded-Zr	2.1 - 2.9	Max 0.3	Max 0.4	Max 0.2	5.1 - 6.1	Max 0.5	1.2- 2	Balance
AA7075-rolled-Zr	2.1 - 2.9	Max 0.3	Max 0.4	Max 0.2	5.1 - 6.1	Max 0.5	1.2- 2	Balance
AA7075-rolled-ZnPh-sealer	2.1 - 2.9	Max 0.3	Max 0.4	Max 0.2	5.1 - 6.1	Max 0.5	1.2- 2	Balance
AA7075-rolled-ZnPh-no sealer	2.1 - 2.9	Max 0.3	Max 0.4	Max 0.2	5.1 - 6.1	Max 0.5	1.2- 2	Balance

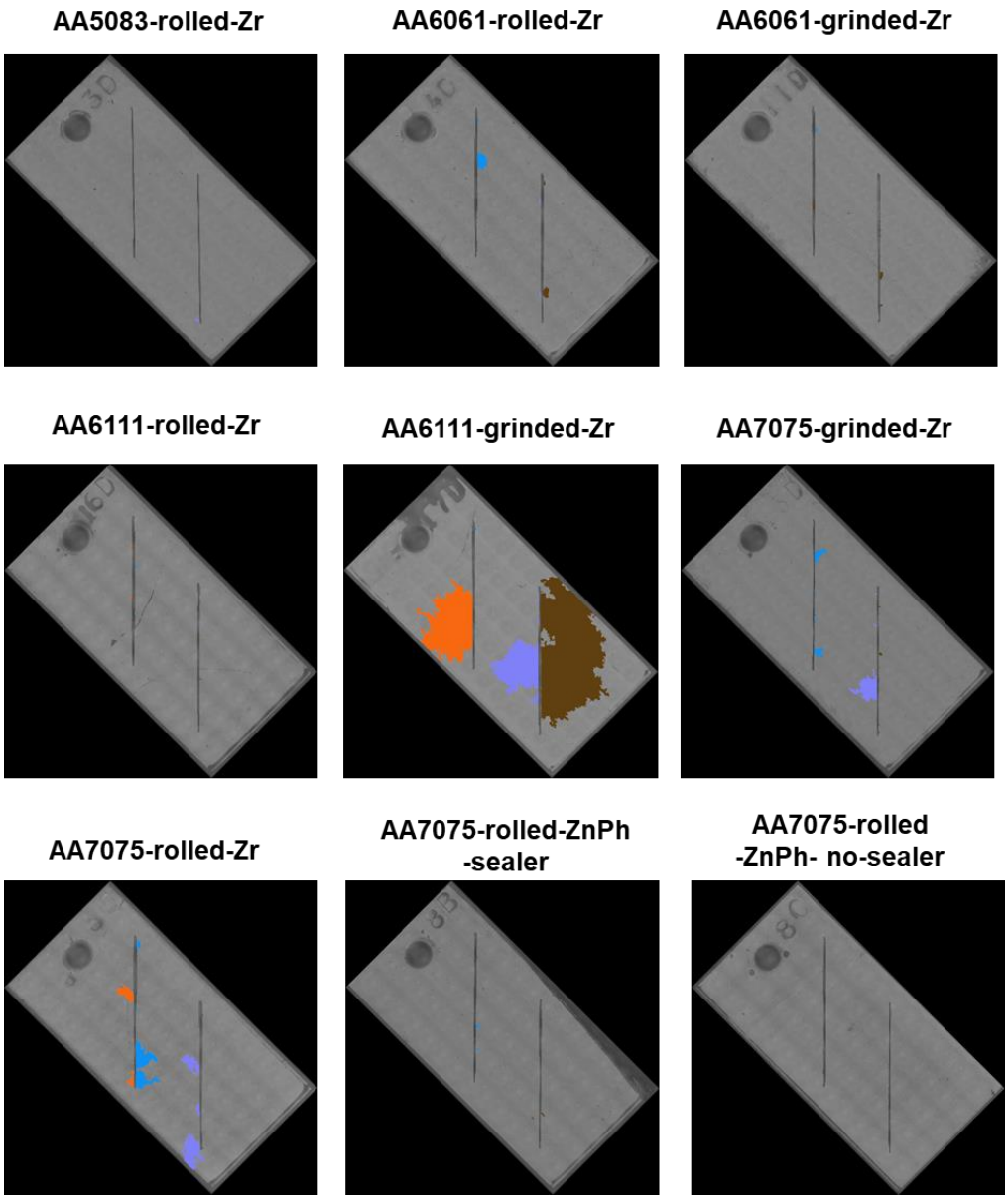

Figure S3. Optical images post road corrosion test for all the nine differently finished AAxxxx surfaces, the colored areas depict corrosion islands resulting from the 2 years of exposure on Canadian roads under varying weather conditions.

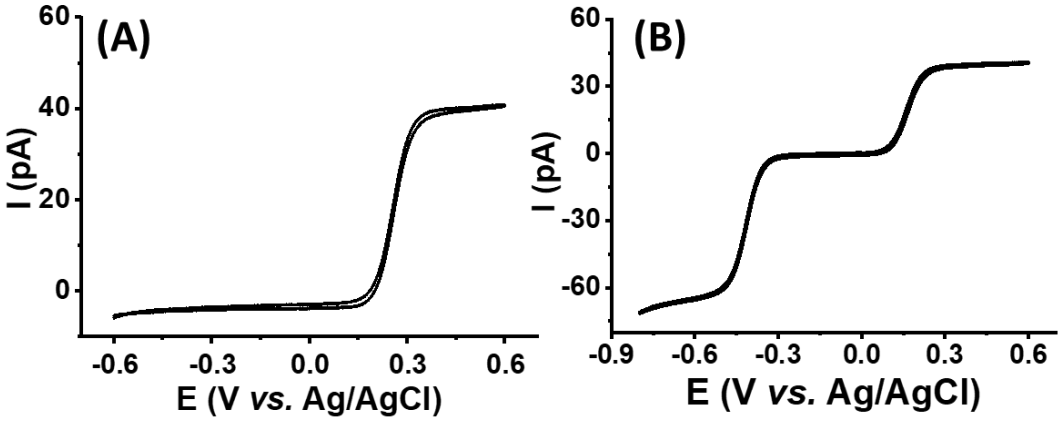

Figure S4. Cyclic voltammetry measurements collected in EG-OH electrolyte solution composed of 35gNaCl / L EG-OH and a redox mediator/its mixture, (A) 1 mM FcMeOH and (B) equimolar mixture of FcMeOH and RuHex at a scan rate of 10 mV s^{-1}.

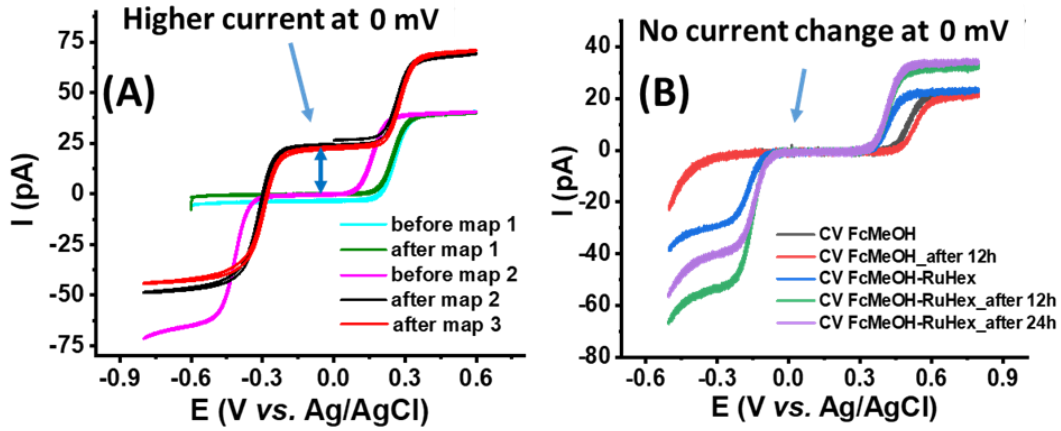

Figure S5. Cyclic voltammetry measurements on (A) Al sample before and after map 2 & map 3, and (B) a plastic substrate while continuously polarising the tip for the same duration and potential, which is required for map 1, map 2 and map 3. All the measurements were performed at a scan rate of 10 mV s^{-1}.

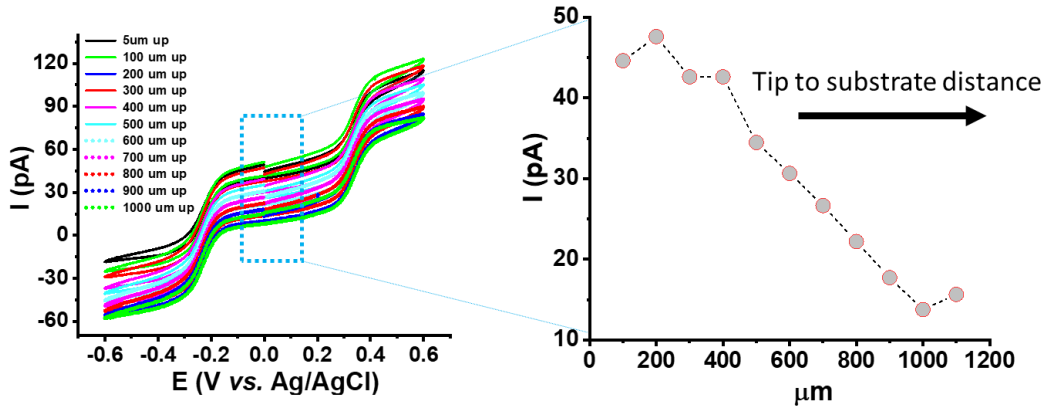

Figure S6. Cyclic voltammetric measurements post three SECM maps. Left graph shows the CV response at various tip-to-substrate distances in an equimolar mixture of FcMeOH and RuHex in the electrolyte (35gNaCl / L EG-OH). Right graph shows the current response at 0 mV (data from the left graph) vs. retracted distance showing variation in current response originating from the initial local accumulation of locally produced Ru^{2+}.

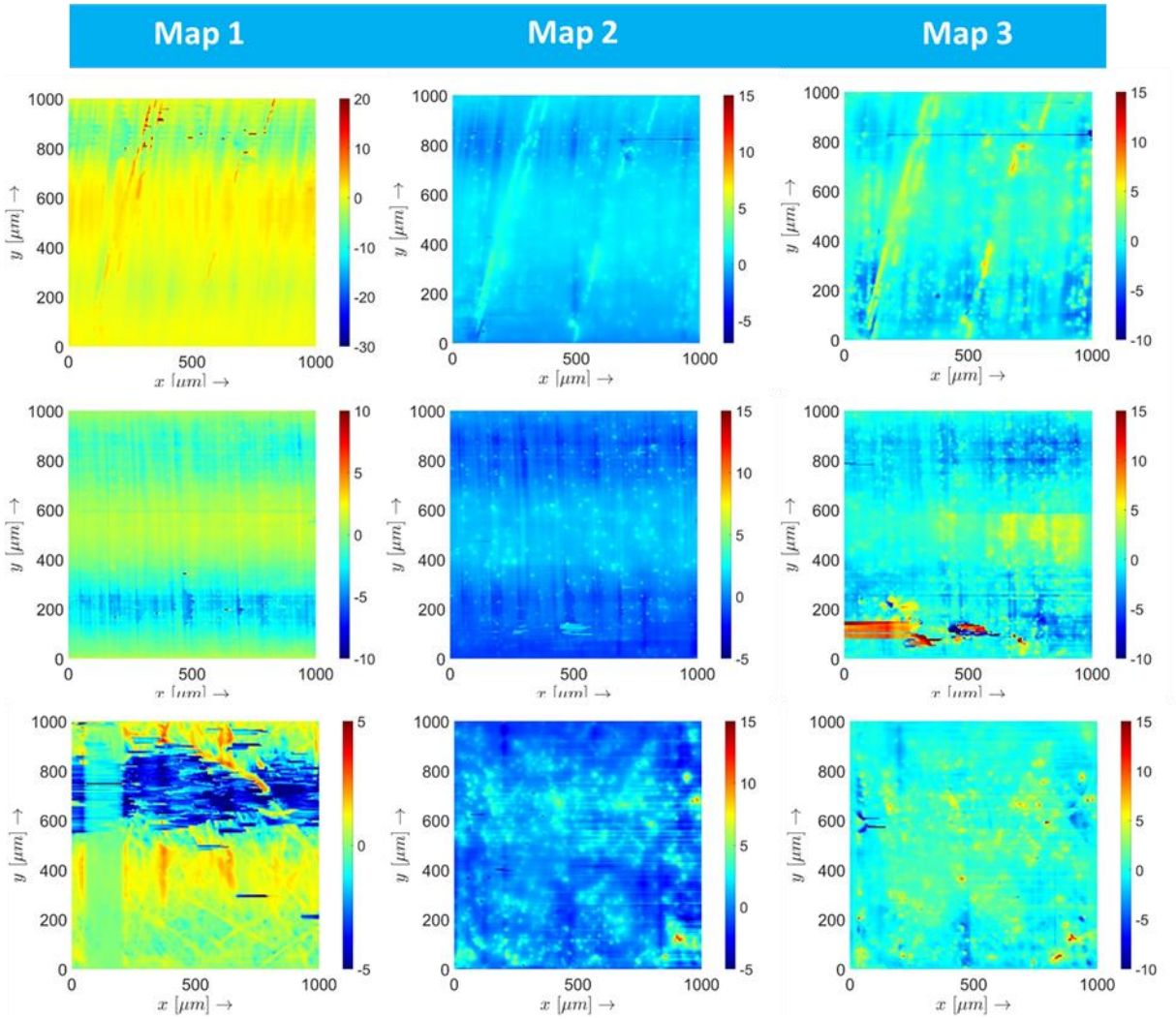

Figure S7. SECM mapping on three samples namely, AA5083-rolled-Zr (top row), AA6061-rolled-Zr (middle row), and AA6061-grinded-Zr (bottom row). The images in the three columns represent three types of SECM mapping performed, left for Map 1, middle for Map 2, and right for Map 3 for the three samples respectively.

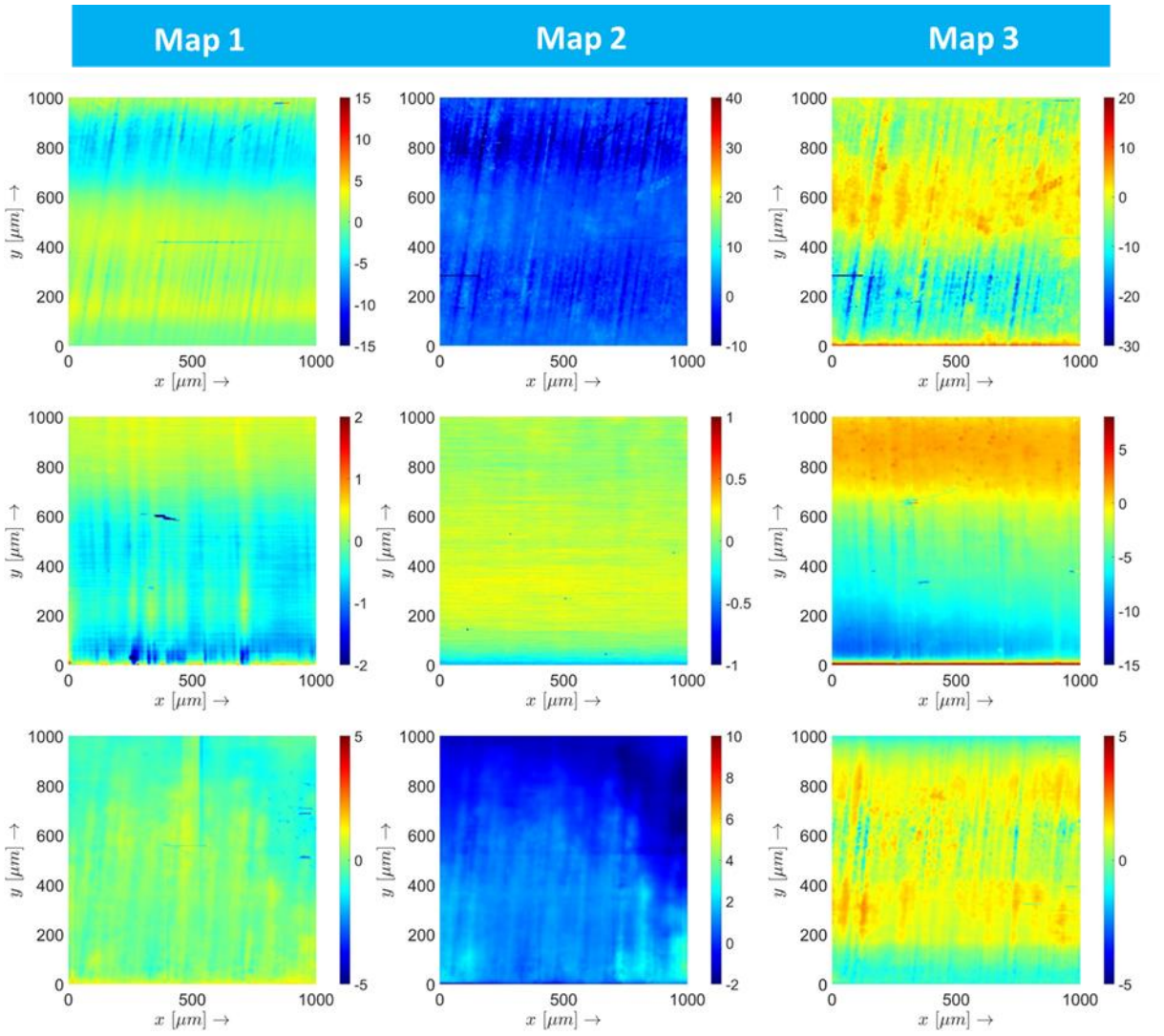

Figure S8. SECM mapping on three samples namely, AA7075-rolled-Zr (top row), AA7075-rolled-ZnPh-sealer (middle row), and AA7075-rolled-ZnPh-no-sealer. The images in the three columns represent three types of SECM mapping performed, left for Map 1, middle for Map 2, and right for Map 3 for the three samples respectively.

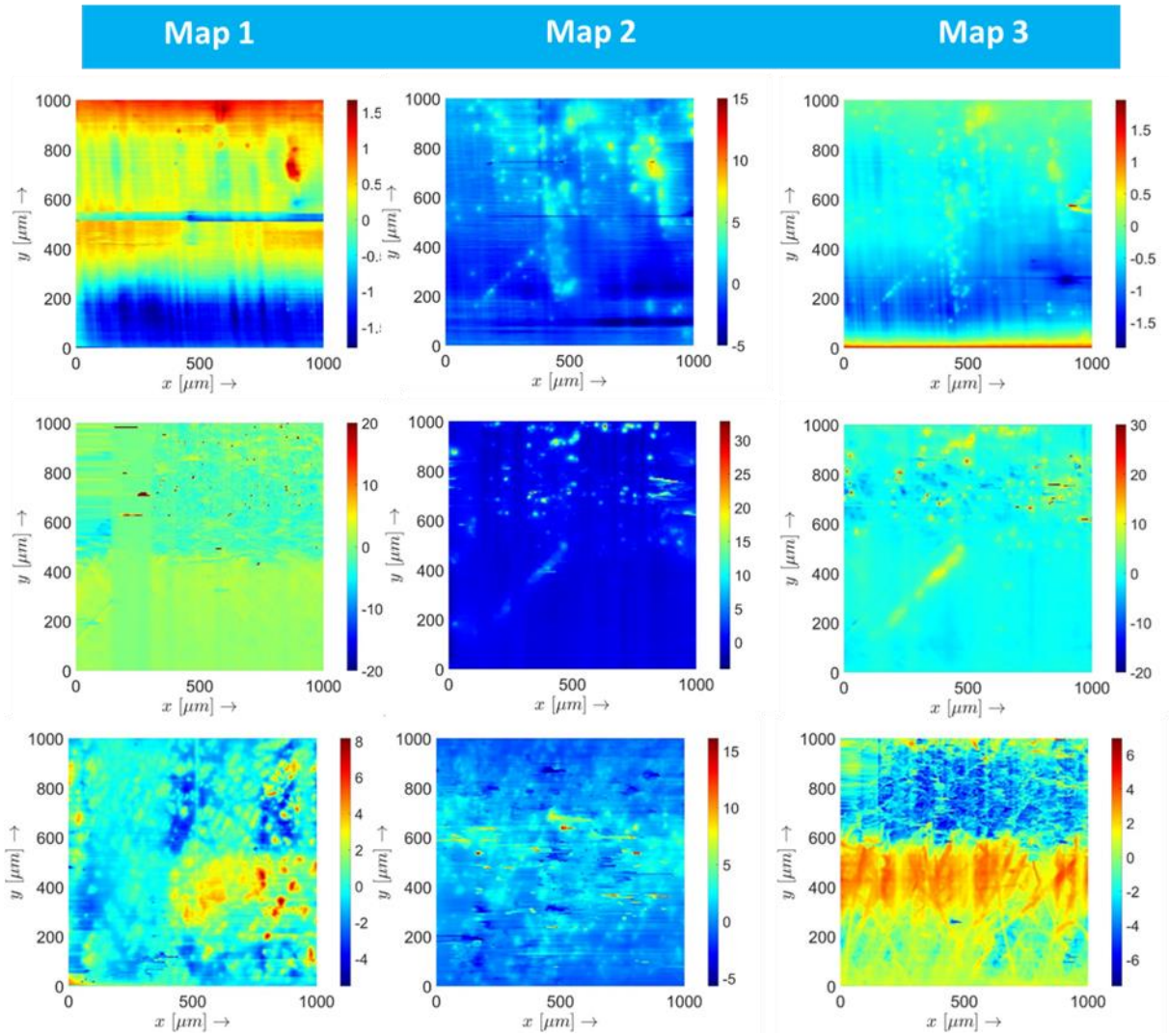

Figure S9. SECM mapping on three samples namely, AA6111-rolled-Zr (top row), AA6111-grinded-Zr (middle row), and AA7075-grinded-Zr (bottom row). The images in the three columns represent three types of SECM mapping performed, left for Map 1, middle for Map 2, and right for Map 3 for the three samples respectively.

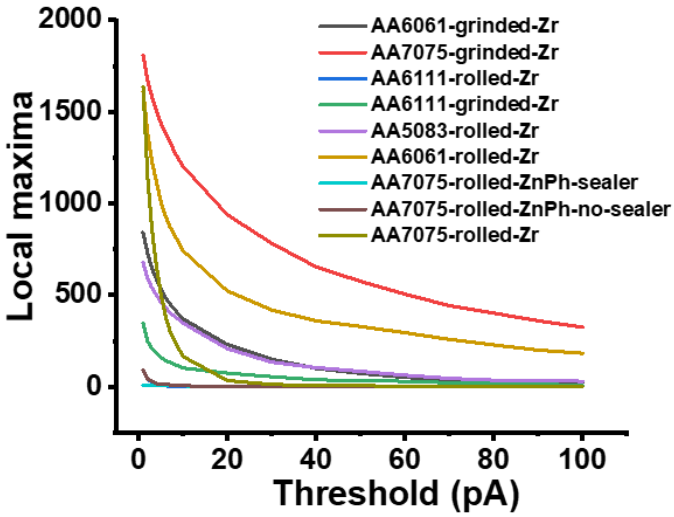

Figure S10. Variation of local maxima w.r.t. threshold current (pA) in map 2 for all the nine samples.

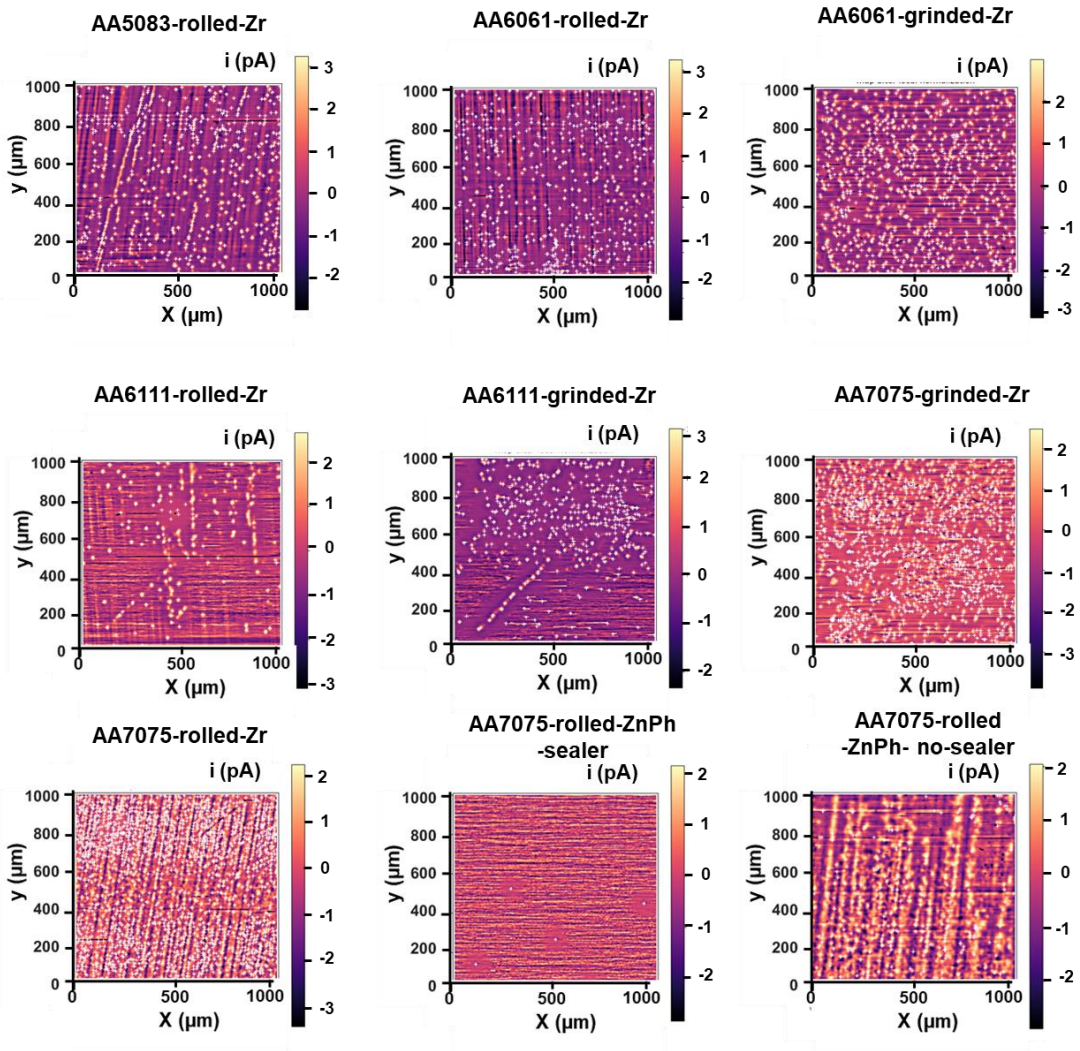

Figure S11. SECM map 2 for all the nine AAxxxx samples with an overlay of identified corrosion hotspots from 'findmaxima2d' function (description in Experimental section).

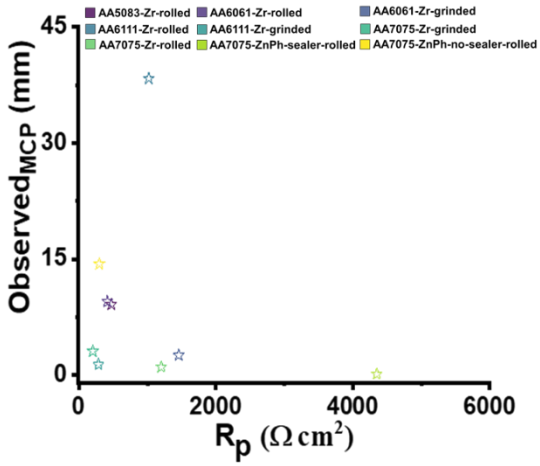

Figure S12. Represents the relationship between observed MCP (road test) and Rp (bulk scale measurements). No clear correlation was found between the bulk corrosion testing parameters and road test results.

Reference:

(1) Sun, Z.; Liang, C.; Chen, Y.; Ma, Z.; Li, Q.; Yin, Z.; Ling, Y.; Xu, Y.; Liu, Z. Corrosion Characteristics and Prediction Model of Aluminum Alloys in Saturated Na2SO4 Solution. *Mater. Chem. Phys.* **2023**, *308* (March), 128273.

(2) You, X.; Xing, Z.; Jiang, S.; Zhu, Y.; Lin, Y.; Qiu, H.; Nie, R.; Yang, J.; Hui, D.; Chen, W.; Chen, Y. A Review of Research on Aluminum Alloy Materials in Structural Engineering. *Dev. Built Environ.* **2024**, *17* (April), 100319.

(3) Environmental Canada, https://weather.gc.ca/en/location/index.html?coords=46.811,-71.225, (accessed on October 01, 2024)

(5) Danis, L.; Polcari, D.; Kwan, A.; Gateman, S. M.; Mauzeroll, J. Fabrication of Carbon, Gold, Platinum, Silver, and Mercury Ultramicroelectrodes with Controlled Geometry. *Anal. Chem.* **2015**, *87* (5), 2565–2569.

(5) ASM Aerospace Spefification Metals Inc., https://asm.matweb.com/search/SpecificMaterial.asp?bassnum=ma7075t6, (accessed on June 12th , 2024)

(6) J. D. Hunter, *Comput. Sci. Eng.* **2007**, *9*, 90–95.

(7) D. Sage and M. Unser, *Proceedings 2001 International Conference on Image Processing (Cat. No.01CH37205)*, Thessaloniki, Greece, **2001**,3, pp. 298-301.

(8) S. Misra, Y. Wu, *Machine Learning Assisted Segmentation of Scanning Electron Microscopy Images of Organic-Rich Shales with Feature Extraction and Feature Ranking*, Elsevier Inc., **2019**. pp 289-315.